Interpretation of the auto-mutual information rate of decrease in the context of biomedical signal analysis

Interpretation of the auto mutual information rate of decrease in the context of biomedical signal analysis. Application to electroencephalogram recordings

Javier Escudero, Roberto Hornero and Daniel Abásolo

Biomedical Engineering Group, E.T.S.I. Telecomunicación, University of Valladolid, Camino del Cementerio s/n, 47011, Valladolid (Spain)

E-mail: javier.escudero@ieee.org

Abstract
The mutual information (*MI*) is a measure of both linear and non-linear dependences. It can be applied to a time series and a time-delayed version of the same sequence to compute the auto mutual information function (*AMIF*). Moreover, the *AMIF* rate of decrease (*AMIFRD*) with increasing time delay in a signal is correlated with its entropy and has been used to characterise biomedical data. In this paper, we aimed at gaining insight into the dependence of the *AMIFRD* on several signal processing concepts and at illustrating its application to biomedical time series analysis. Thus, we have analysed a set of synthetic sequences with the *AMIFRD*. The results show that the *AMIF* decreases more quickly as bandwidth increases and that the *AMIFRD* becomes more negative as there is more white noise contaminating the time series. Additionally, this metric detected changes in the non-linear dynamics of a signal. Finally, in order to illustrate the analysis of real biomedical signals with the *AMIFRD*, this metric was applied to electroencephalogram (EEG) signals acquired with eyes open and closed and to ictal and non-ictal intracranial EEG recordings.

Keywords: Auto mutual information, biomedical signal analysis, electroencephalogram, non-linear analysis, signal regularity

PACS number(s): 05.45.Tp; 87.10.Vg; 87.85.Ng

1. Introduction

Several physiological signals, including cardiovascular and brain activity recordings, exhibit a partially non-linear behaviour (Andrzejak *et al* 2001, Hoyer *et al* 2002, Palacios *et al* 2007). Additionally, some authors have suggested that healthy systems have non-linear complex relationships that fail with ageing and disease (Costa *et al* 2005, Goldberger *et al* 2002). In this context, Information theory (Shannon and Weaver 1949) may provide a unique framework to statistically assess information taking into account non-linear features. One of the concepts derived from this theory is mutual information (*MI*). *MI* measures statistical dependence between and within signals and can be useful to characterise and analyse time series. This statistic estimates the information gained from observations of one random event on another (Cellucci *et al* 2005, Fraser and Swinney 1986, Pompe *et al* 1998). It evaluates both linear and non-linear dependences between two time series (Fraser and Swinney 1986, Pompe *et al* 1998). Hence, this metric is a non-linear, complementary counterpart to the classical correlation

(Abarbanel *et al* 1993, Hoyer *et al* 2005, Pompe *et al* 1998). As function of a time delay, τ, the *MI* can be applied to time-delayed versions of two different signals (cross mutual information function) or from the same sequence (auto mutual information function) (Hoyer *et al* 2005, Pompe *et al* 1998). Following the notation by Pompe *et al* (1998) and Hoyer *et al* (2002), these functions will be denoted *CMIF* and *AMIF*, respectively.

The concept of *MI* has been widely applied in biomedical signal analysis to evaluate the dependence between different biomedical recordings (Hinrichs *et al* 2008, Hoyer *et al* 2005, 2007, Palacios *et al* 2007, Pompe *et al* 1998). This application is based on the fact that the *MI* quantifies the linear and non-linear statistical coupling between signals. Thus, it can be a useful tool to quantify synchronization (David *et al* 2004, Pompe *et al* 1998, Quian Quiroga *et al* 2002). In biomedical signal analysis, the *CMIF* of respiratory and heart rate variability recordings provides useful information to detect cardiac and respiratory diseases (Alonso *et al* 2007, Hoyer *et al* 2002). The statistical dependences between different brain regions have also been assessed with *MI* techniques in several brain states (Hinrichs *et al* 2008, Huang *et al* 2003, Min *et al* 2003, Teplan *et al* 2006, Xu *et al* 1997) and neurological disorders, like Alzheimer's disease (Benedetti *et al* 2006, Jeong *et al* 2001) or schizophrenia (Na *et al* 2002).

The *AMIF* rate of decrease (*AMIFRD*) with increasing time delay is correlated with signal entropy (Paluš 1996). Thus, the decay of the *AMIF* may be considered a measure of signal predictability (Fraser and Swinney 1986, Jeong *et al* 2001, Palacios *et al* 2007). It has been previously shown that the *AMIFRD* provides relevant information about the underlying physiological systems (Hoyer *et al* 2005). This metric has been applied to study several patho-physiological conditions. For example, the *AMIFRD* of electroencephalogram (EEG) and magnetoencephalogram (MEG) recordings characterised patients with Alzheimer's disease in contrast to control subjects (Abásolo *et al* 2008, Jeong *et al* 2001, Gómez *et al* 2007). This metric also shows differences between the EEG of schizophrenic patients and that recorded from control subjects (Na *et al* 2002). In addition, different *AMIF* decay parameters can help to detect several cardiomyopathies from cardiac data (Hoyer *et al* 2002, 2005, Palacios *et al* 2007).

Due to the relevance and the possible usefulness of the *AMIFRD* in various biomedical analyses, it is important to understand and exemplify the behaviour of this metric for diverse kinds of signals. It is worth mentioning that several studies have illustrated the behaviour of the *CMIF* for some test sequences in contrast to the correlation function (David *et al* 2004, Hoyer *et al* 2002, Paluš *et al* 1993, Pompe *et al* 1998, Quian Quiroga *et al* 2002). Moreover, the decay of the *AMIF* has been compared with other entropic measures (Abásolo *et al* 2008, Hoyer *et al* 2005). Following these research works, this study aims at pointing out the relationships between the *AMIFRD* and straightforward signal characteristics like noise power or non-linear dynamics to gain a better understanding of this metric. Furthermore, we want to illustrate the application of the *AMIFRD* to biomedical signals by analyzing real surface and intracranial EEG data.

2. Auto mutual information function rate of decrease (*AMIFRD*)

MI is based on concepts from Information theory (Shannon and Weaver 1949). Let $X(t)=\{x(1),x(2),\ldots,x(T)\}$ be a sequence acquired from a stochastic process (Alonso *et al* 2007). If the amplitude values of the variable $X(t)$ are partitioned into *I* bins, a probability $p_i^X = n_i^X / T$ can be assigned to each possible partition $X_i(i=1,\ldots,I)$, where n_i^X is the number of samples in X_i (David *et al* 2004, Gómez *et al* 2007). Shannon's entropy for $X(t)$, which is denoted by $H(X)$, is the average amount of information gained from any observation of $X(t)$ (Shannon and Weaver 1949):

$$H(X) = -\sum_i p_i^X \log_2\left(p_i^X\right). \quad (1)$$

Let $X(t)$ be coupled with another signal, $Y(t)$, which was measured and found in a partition bin $Y_j(j=1,\ldots,J)$ with an associated probability $p_j^Y = n_j^Y / T$, where n_j^Y is the number of samples in Y_j. Then, the uncertainty about $X(t)$ is (Jeong *et al* 2001):

$$H\left(X\left|Y_j\right.\right) = -\sum_i \frac{p_{ij}^{XY}}{p_j^Y} \log_2\left(\frac{p_{ij}^{XY}}{p_j^Y}\right), \tag{2}$$

where p_{ij}^{XY} is the joint probability for the partitions X_i and Y_j of the variables $X(t)$ and $Y(t)$, in that order. The mean uncertainty of $X(t)$, under the condition that $Y(t)$ is known, is computed averaging $H\left(X\left|Y_j\right.\right)$ over p_j^Y (Min *et al* 2003):

$$H\left(X\left|Y\right.\right) = \sum_j p_j^Y H\left(X\left|Y_j\right.\right) = -\sum_{i,j} p_{ij}^{XY} \log_2\left(\frac{p_{ij}^{XY}}{p_j^Y}\right) = H\left(X,Y\right) - H\left(Y\right) \tag{3}$$

where

$$H\left(X,Y\right) = -\sum_{i,j} p_{ij}^{XY} \log_2\left(p_{ij}^{XY}\right). \tag{4}$$

MI estimates the information obtained from measurements of one event on another – i.e., the reduction in the uncertainty of $X(t)$ when $Y(t)$ is known – (Cellucci *et al* 2005, Fraser and Swinney 1986, Pompe *et al* 1998):

$$MI\left(X,Y\right) = H\left(X\right) - H\left(X\left|Y\right.\right) = H\left(X\right) + H\left(Y\right) - H\left(X,Y\right), \tag{5}$$

which can be rewritten as (Gómez *et al* 2007, Jeong *et al* 2001, Na *et al* 2002):

$$MI\left(X,Y\right) = \sum_{i,j} p_{ij}^{XY} \log_2\left(\frac{p_{ij}^{XY}}{p_i^X p_j^Y}\right). \tag{6}$$

This expression represents the cross mutual information between $X(t)$ and $Y(t)$. It is zero when $X(t)$ and $Y(t)$ are statistically independent (Chapeau-Blondeau 2007, Hoyer *et al* 2002). The $CMIF(\tau)$ is obtained estimating p_{ij}^{XY} and p_j^Y from successive time-delayed versions of $Y(t)$: $Y(t+\tau)$ (Hoyer *et al* 2002, Jeong *et al* 2001, Na *et al* 2002, Xu *et al* 1997). Similarly, $AMIF(\tau)$ is computed replacing $Y(t+\tau)$ with time-delayed versions of $X(t)$, $X(t+\tau)$ (Gómez *et al* 2007, Jeong *et al* 2001):

$$AMIF\left(\tau\right) = \sum_{i,j} p_{ij}^{X(t)X(t+\tau)} \log_2\left(\frac{p_{ij}^{X(t)X(t+\tau)}}{p_i^{X(t)} p_j^{X(t+\tau)}}\right). \tag{7}$$

The $AMIF(\tau)$ measures statistical predictability within a signal, that is, the predictability of $X(t+\tau)$ from $X(t)$ (Gómez *et al* 2007, Jeong *et al* 2001). It is based on the amplitude distributions of $X(t)$ on different time scales, τ (David *et al* 2004). These amplitude distributions are estimated from histograms (Abásolo *et al* 2008, Alonso *et al* 2007, Gómez *et al* 2007, Jeong *et al* 2001).

Before estimating the histograms, a ranking transformation was applied to the time series $X(t)$ and $X(t+\tau)$ (Alonso *et al* 2007, Hoyer *et al* 2002, Pompe *et al* 1998). This ranking transformation from $X(t)$ to $X^*(t)$ is given by:

$$X^*(t) = \frac{1}{T} N\left\{t^* : X\left(t^*\right) < X(t),\ t^* = 1,2,\ldots,T\right\}, \tag{8}$$

where $N\{\cdot\}$ denotes the cardinality (the number of elements) in the set (Alonso *et al* 2007, Pompe *et al* 1998). This transformation replaces the real values of $X(t)$ with their ranks, that is, T times $X^*(t)$ is the number of values in the original time series that are less than $X(t)$. Then, these values are divided by T, so that the transformed sequence is always uniformly distributed in the interval $[0,1)$ (unit interval) (Pompe *et al* 1998). However, if and only if the multivariate ranked series ($X^*(t), X^*(t+\tau)$) have a uniform 2D-distribution, $X^*(t)$ and $X^*(t+\tau)$, and thus the original sequences $X(t)$ and $X(t+\tau)$, are statistically independent (Pompe *et al* 1998). Thanks to this partition of the plane ($X(t), X(t+\tau)$), the estimation of the *MI* is more robust against outliers and artefacts in data (Alonso *et al* 2007, Cellucci *et al* 2005).

For a fixed sequence length, the estimations of the average probabilities are more accurate when larger bins are used to construct the histograms. However, the joint probability distribution could be too flat and the *MI* may be underestimated. On the other hand, smaller partitions may enhance the changes in the joint probability distribution over short distances, but they produce fluctuations due to the small sample size. Thus, *MI* may be overestimated (Fraser and Swinney 1986, Jeong *et al* 2001). Very different criteria have been suggested in the literature to estimate the partition size used to construct the histograms (Cellucci *et al* 2005). In this study, the influence of the number of bins in the *AMIFRD* was inspected by computing this metric for the synthetic signals described in Section 3.1 using histograms with I = 8, 16, 32, 64 and 128 partitions.

The $AMIF(\tau)$ was estimated over a time delay from $\tau = 0$ to $\tau = 0.5$ s. This time lag has been previously used in several analyses of brain activity (Abásolo *et al* 2008, Gómez *et al* 2007, Jeong *et al* 2001, Min *et al* 2003, Na *et al* 2002). Moreover, the $AMIF(\tau)$ was normalized so that $AMIF(\tau = 0) = 1$ before computing the *AMIFRD* (Abásolo *et al* 2008, Gómez *et al* 2007, Jeong *et al* 2001, Na *et al* 2002). It should be noticed that for $\tau = 0$ the $AMIF(\tau = 0)$ is computed between two identical sequences: $X(t)$ and $X(t+0)$. Thus, regardless of the analysed time series, it is fulfilled that (Hoyer *et al* 2002, Quian Quiroga *et al* 2002):

$$AMIF(\tau = 0) = H(X). \tag{9}$$

Moreover, given the fact that a ranking transformation was applied to uniformly distribute the signal samples in the unit interval:

$$AMIF(\tau = 0) = \log_2(I), \tag{10}$$

where, as mentioned earlier, I denotes the number of partitions used to estimate the histogram of $X(t)$ (Hoyer *et al* 2002, 2005, 2006).

The *AMIFRD* between $\tau = 0$ and the first relative minimum value was calculated as the slope of the line that fits the $AMIF(\tau)$ in a least-squares sense (Abásolo *et al* 2008, Gómez *et al* 2007, Jeong *et al* 2001). Therefore, different time scales were simultaneously considered when analysing the signal. This methodology can be useful when no information is known in advance about the prominent time scales of a signal, as it often occurs in biomedical applications (Hoyer *et al* 2005, Palacios *et al* 2007). This rate of decrease measures the information loss versus τ (Hoyer *et al* 2002) and it is correlated with signal entropy (Abásolo *et al* 2008, Paluš 1996).

3. Study and application of the *AMIFRD*

3.1. Synthetic signals

This section describes the simulated signals used to study the *AMIFRD* in terms of simple concepts like additive noise power or non-linear dynamics. All these synthetic signals had a length of 150 s and their sampling frequency (f_s) was 150 Hz. Hence, they had 22500 sample points. These simulated time series are illustrated in figure 1, which shows their spectrogram, time plot and two zooms on the first and last time intervals to illustrate the changes in the signal characteristics.

3.1.1. Test a: MIX process

This test analysed how the evolution from a stochastic signal to a periodic deterministic sequence affected the *AMIFRD*. For this purpose, we created a *MIX* process used in previous studies (Ferrario *et al* 2006, Pincus 1991). It is defined as:

$$MIX = (1-z)x + z\,y, \tag{11}$$

where z is a random variable which is equal to 1 with probability p and equal to 0 with probability $1 - p$, x is a periodic sequence generated by $x_k = \sqrt{2}\sin(2\pi k/12)$, and y is a uniformly distributed variable on $\left[-\sqrt{3},\sqrt{3}\right]$ (Ferrario *et al* 2006, Pincus 1991). The synthetic signal was based on a *MIX* process whose parameter p varied from 0.9 to 0.1 linearly. Hence, this sequence, which is shown in figure 1(a), evolved from randomness to orderliness.

3.1.2. Test b: Quasi-periodic signal plus noise

The objective of this test was to find out whether the *AMIFRD* is sensitive to changes in power of noise added to quasi-periodic signals. Thus, we generated an amplitude-modulated quasi-periodic signal with additive white Gaussian noise of diverse power. This sequence is similar to that used in Aboy *et al* (2006) or Hornero *et al* (2005). The time series was created as an amplitude-modulated sum of two sine waves with frequencies at 0.61 Hz and 1 Hz. The first 30 s of this sequence were noise-free. Afterwards, white Gaussian noise was added to the signal, with the noise power increasing every 15 s. Figure 1(b) plots this time series.

3.1.3. Test c: Autoregressive process

In this test, the dependence between the *AMIFRD* and the spectral content of coloured noise was studied. An autoregressive process of order 1 – $AR(1)$ – was created varying the model parameter, ρ, from +0.9 to –0.9 linearly. Thus, its energy moved from low to high frequencies. When ρ was equal to 0, the sequence corresponded to Gaussian white noise. Figure 1(c) depicts the corresponding spectrogram, time plot and zoom views.

3.1.4. Test d: Logistic map

This test aimed at determining whether the *AMIFRD* is able to detect changes from periodic to chaotic behaviour in a signal. This analysis was based on the logistic map, which depends on the model parameter μ (Ferrario *et al* 2006, Pincus 1991):

$$x_k = \mu x_{k-1}(1 - x_{k-1}). \tag{12}$$

The synthetic signal was composed by 2 segments of 11250 data points. The first one was generated with μ = 3.55. With this parameter, the time series oscillated among 8 values (Baker and Gollub 1990). The second segment was computed with μ = 3.60 in order to create chaotic oscillations (Baker and Gollub 1990). Figure 1(d) exemplifies this simulated signal.

3.1.5. Test e: Lorenz system

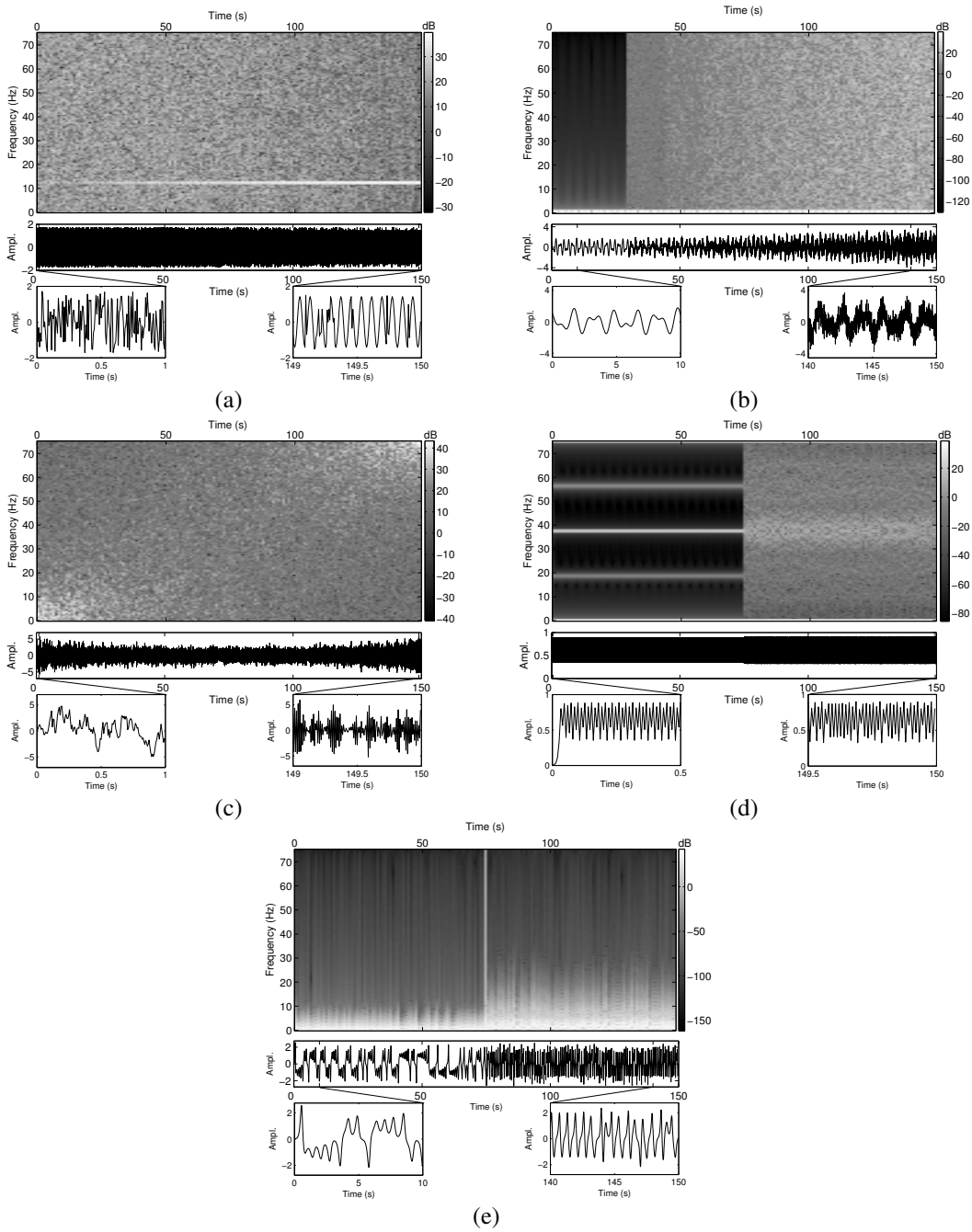

Figure 1. Spectrograms, time plots and zoom views on the first and last time intervals of the synthetic signals. (a) Test a: *MIX* process which evolves from randomness to periodic oscillations. (b) Test b: Quasi-periodic signal with increasing additive noise power. (c) Test c: *AR*(1) process with variable parameter. (d) Test d: Logistic map divided into periodical and chaotic parts. (e) Test e: Lorenz system with two different non-linear dynamics.

In this test, we studied whether the *AMIFRD* detects changes in the behaviour of a non-linear system like the Lorenz attractor, which is given by:

$$\begin{aligned} \dot{x} &= \sigma(y - x) \\ \dot{y} &= x(\rho - z) - y \\ \dot{z} &= xy - \beta z \end{aligned} \tag{13}$$

where σ, β and ρ are the system parameters (Baker and Gollub 1990, Kantz and Schreiber 1997). The first segment of this synthetic sequence had a length of 11250 samples and it was generated with $\sigma = 10$, $\beta = 8/3$ and $\rho = 28$. Thus, it exhibited a chaotic behaviour. The second segment also

had 11250 points and was created with $\sigma = 10$, $\beta = 8/3$ and $\rho = 99.96$, which produced a torus knot (Baker and Gollub 1990, Kantz and Schreiber 1997). Both parts were generated using a fixed step-size first order integration method without pre-integration and with the step-size set to $1/f_s$. After the two parts had been created, they were normalized so that their standard deviation was equal to 1. Figure 1(e) displays the coordinate x, which was the time series analysed in this study.

3.2. Evolution with signal parameters

For every kind of synthetic signal, 250 independent realizations of the time series were created with different initial phases or random seeds. Then, for each of these independent realizations, the *AMIFRD* was computed in a moving window of 30 s (4500 data samples) with 90% overlap and $I = 8$, 16, 32, 64 and 128 partitions to construct the histograms. The 250 rates of decrease were averaged for each window. Therefore, we could test whether the *AMIFRD* is sensitive to changes in the signal parameters varied in this study.

3.3. Distribution of the AMIFRD for different kinds of signals

In addition to test how the *AMIFRD* changes with some signal parameters, we also studied its variability for three different kinds of sequence. We generated 10000 independent realizations of: 1) a logistic map with $\mu = 4$ (non-linear oscillator) (Hoyer *et al* 2002); 2) an $AR(1)$ process with $\rho = +0.9$ (low-frequency linear oscillator) and 3) an $AR(1)$ process with $\rho = -0.9$ (high-frequency linear oscillator). All these time series had a length of 30 s with $f_s = 150$ Hz (4500 sample points). The *AMIF* was computed with the number of bins that provided the most sensitive estimations to the changes in the synthetic signal parameters.

3.4. Application to real EEG recordings

Finally, the *AMIFRD* was applied to five groups of real EEG signals in order to illustrate the analysis of real biomedical time series with this metric. These recordings belong to the EEG database made available online by Andrzejak *et al* (2001) at the Department of Epileptology, University of Bonn. This section only describes these signals briefly.

Each of the five datasets contains 100 single-channel EEG signals of 23.6 s recorded with $f_s = 173.61$ Hz (4096 sample points). Subsets A and B contain surface EEG signals recorded from five healthy volunteers who were relaxed in an awake state. Whereas the subjects had their eyes open during the recording of the EEG in dataset A, the EEG signals of dataset B were acquired with eyes closed (Andrzejak *et al* 2001). The *AMIFRD* was also computed for three subsets (C, D and E) of intracranial EEG recordings from five epileptic patients, who had achieved complete seizure control after a surgical procedure (Andrzejak *et al* 2001). Signals in set D were recorded within the epileptogenic zone, whereas the EEGs of set C were acquired from the opposite brain hemisphere. Sets C and D contained only activity measured during seizure free intervals. On the other hand, set E was only composed of seizure activity recorded from all sites exhibiting ictal activity. Additional details can be found in Andrzejak *et al* (2001).

The *AMIFRD* was calculated using the number of partitions considered optimal after the simulated signals analyses. Prior to these computations, all EEG epochs were digitally filtered using a FIR band-pass filter with cut-off frequencies at 0.5 Hz and 40 Hz.

4. Results and discussion

This study aimed at characterising the behaviour of the *AMIFRD* in terms of straightforward signal processing concepts. In order to do so, we analysed different kinds of synthetic signals with the *AMIFRD* using $I = 8$, 16, 32, 64 and 128 bins to calculate the histograms. These results are depicted in figure 2. Despite the fact that the *MI* value may be under- or over-estimated depending on the number of bins used to construct the histograms, figure 2 shows that the average *AMIFRD*s are relatively stable for a range of I values. On the one hand, the *AMIFRD*

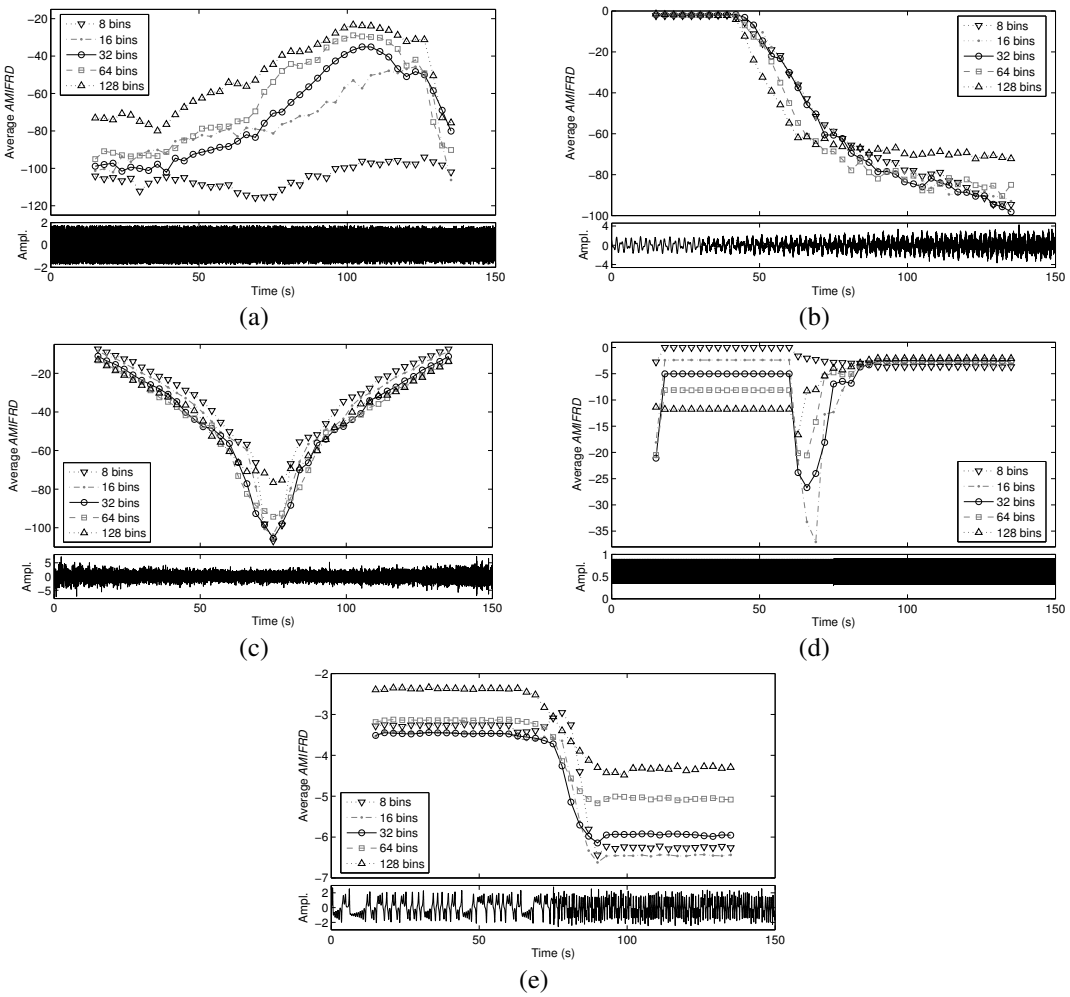

Figure 2. Average results of the *AMIFRD* computed from the tests signals using I = 8, 16, 32, 64 and 128 bins to construct the histograms. (a) Test a: *AMIFRD* versus signal randomness. (b) Test b: Evolution of the *AMIFRD* with additive noise power. (c) Test c: Evolution of the *AMIFRD* with signal spectral content. (d) Test d: Relationship between the *AMIFRD* and periodic or chaotic behaviour. (e) Test e: *AMIFRD* versus two different types of non-linear dynamics.

computed with 8 partitions was unable to show the changes in signal parameters in tests a and test d. On the other hand, in tests c and e, this metric provided less differences with I = 128 than with I = 16, 32 or 64 bins. Furthermore, the evolution of the *AMIFRD* for the studied signal parameters was similar when 16, 32 and 64 partitions were used to build the histograms. Thus, considering the results obtained with these test signals, the remaining analyses will be carried out using histograms of 32 bins.

The results of the test that aimed to determine whether the evolution from randomness to deterministic oscillations affects the *AMIFRD* are plotted in figure 2(a). This parameter detects changes in the content of a signal when it changes from randomness to orderliness.

In figure 2(b), it can be seen that the *AMIFRD* is sensitive to changes in additive noise power, becoming more negative as noise power increases. Despite the fact that the ranking transformation made the *AMIFRD* robust to artefacts in the signals (Alonso *et al* 2007), figure 2(b) indicates that this parameter depends on the signal-to-noise ratio (*SNR*) for quasi-periodic signals. Consequently, we can infer that the *AMIFRD*, even when the ranking transformation is applied, tends to saturate for low *SNR*s, offering the most negative values for completely noisy signals.

Using an $AR(1)$ process, we studied how the *AMIFRD* changed with the signal spectral content. The results are depicted in figure 2(c). This analysis proves that time series with wider spectra (e.g., white noise) produce more negative *AMIFRD*s. On the other hand, time series with

narrower spectral content provide a smoother *AMIF* decay, irrespective of whether their spectra are centred at low or high frequencies. These results agree with a previous study that showed that white noise is more irregular than coloured noise (Hornero *et al* 2005). Figure 2(c) also suggests that the *AMIF* rate of decrease does not clearly distinguish between low or high-frequency noises.

Figure 2(d) shows the results of the test designed to assess how the change from a periodic to a chaotic signal affects the *AMIFRD*. The time series was composed of two segments generated using a logistic map. There is a sudden fluctuation in the *AMIFRD* values when the behaviour of the logistic map becomes chaotic. This fluctuation appears when both kinds of dynamics (periodic oscillations and chaos) are included in the moving window from which the *AMIFRD* is computed. When the moving window comprises only one kind of dynamics, the values of this metric are stable. In agreement with Hoyer *et al* (2002), it can be seen that the *AMIFRD* for white noise is more negative than that related to the logistic map since the former loses more information with τ.

Using the Lorenz system, we could explore whether the *AMIFRD* detects changes in the non-linear equations that govern this system. Figure 2(e) represents our results. It can be observed that the *AMIFRD* values are less negative than those of white noise. Nevertheless, this parameter shows a sudden change between both kinds of non-linear dynamics.

Figure 3 depicts the boxplots of the *AMIFRD* values for 10000 independent realizations of a non-linear (logistic map with $\mu = 4$) and two linear oscillators – $AR(1)$ processes with $\rho = +0.9$ and $\rho = -0.9$. These boxplots show that the ability of the *AMIFRD* to distinguish low- and high-frequency coloured noises is limited. This is due to the fact that the distributions of *AMIFRD* values for the $AR(1)$ processes with $\rho = +0.9$ and $\rho = -0.9$ are similar (p-value = 0.0572, Mann-Whitney U-test). Additionally, it can be noted that the distribution of the *AMIFRD* for the non-linear chaotic oscillator is different from those of the linear $AR(1)$ processes (p-value << 0.0001, Mann-Whitney U-test for the logistic map and the two $AR(1)$ processes).

Figure 4(a) shows the boxplots for the distributions of the *AMIFRD* values obtained from real EEG signals acquired with eyes open and eyes closed. It is well-known that the closed-eyes condition produces certain changes in the EEG. One of the most remarkable alterations is the rise in the power of the alpha rhythm (oscillations between 8 Hz and 13 Hz) (Andrzejak *et al* 2001). Thus, the EEG spectrum is modified in comparison to the eyes-open case. This can be visually observed or studied with spectral analysis methods. Additionally, the boxplots depicted in figure 4(a) show that more negative *AMIFRD* values are related to the eyes-closed state (p-value << 0.0001, Mann-Whitney U-test for subsets A and B of the EEG database). Therefore, we can infer that the closing of eyes is associated with significantly more irregular EEG signals. Multichannel EEG signals recorded with eyes open and closed have also been analysed with other measures based on concepts like complexity and information transfer (Rapp *et al* 2005, Watanabe *et al* 2003). Those results associated the eyes open condition with an increase in algorithmic complexity and a decrease in the Tononi-Edelman complexity, which provided the greatest between-condition statistical significance (Rapp *et al* 2005). However, the diverse results obtained with these measures should be interpreted with care due to the different definitions of the complexity measures applied and the use of multichannel recordings in contrast to the single channel EEG signals analysed here with the *AMIFRD*. Figure 4(b) represents the boxplots for the *AMIFRD* values obtained from the subsets C, D and E of the EEG database. Similarly to the clear visual and spectral changes between ictal and non-ictal activity, there are very significant differences between the *AMIFRD* values computed for these states (p-value << 0.0001, Mann-Whitney U-test for subsets C, D and E of the EEG database). The differences are much more subtle between the inter-ictal EEG activity recorded from the epilogenetic zone and from the opposite brain hemisphere (p-value = 0.0343, Mann-Whitney U-test for subsets C and D).

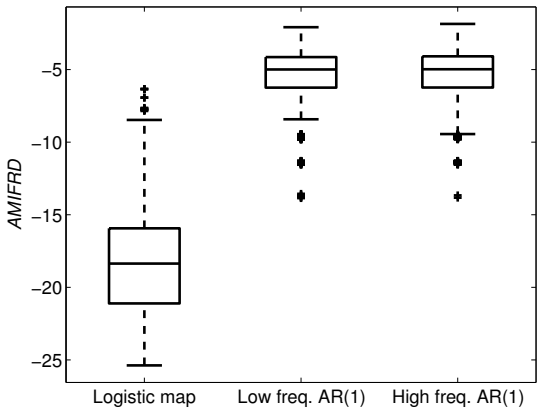

Figure 3. Boxplots representing the distributions of the *AMIFRD* values obtained for 10000 independent realizations of several kinds of signals: a logistic map with $\mu = 4$, an $AR(1)$ model with $\rho = +0.9$ (low frequency) and an $AR(1)$ model with $\rho = -0.9$ (high frequency). A boxplot is composed of a box with three horizontal lines at the lower quartile, median, and upper quartile values and two whiskers, which are lines extending from each end of the boxes to show the extent of the rest of the data. Values beyond the end of the whiskers are considered outliers, which are marked with a "+".

In this study, the *AMIFRD* was estimated using a first-order least-squares fitting method (Abásolo *et al* 2008, Gómez *et al* 2007, Jeong *et al* 2001). Thus, we could assess the information loss on several time scales simultaneously. In contrast, other researchers have estimated *AMIF* decay parameters drawing a straight line between $\tau = 0$ and a certain τ_1 (Na *et al* 2002, Palacios *et al* 2007). In the context of biomedical signal analysis, considering different time scales at the same time can be advantageous in comparison to the use of other non-linear measures based on one time scale only (Costa *et al* 2005). This is due to the fact that physiological mechanisms interoperate at different time scales simultaneously and it is difficult to define a priori a prominent time scale (Hoyer *et al* 2005, Costa *et al* 2005). Furthermore, analysing several time scales may be especially relevant when there is no clear knowledge about the specific time scales associated with the time series (Hoyer *et al* 2005). Thus, variables related to the time evolution of *MI* may be more helpful to characterise a recording than its absolute values (Alonso *et al* 2007).

Our results support the idea that the *AMIFRD*, which is correlated with signal entropy (Abásolo *et al* 2008, Paluš 1996), is an irregularity estimator instead of a complexity measure, as some authors have previously suggested (Jeong *et al* 2001, Na *et al* 2002, Palacios *et al* 2007). From a strict point of view, a quantitative measure of complexity should vanish for both completely ordered and completely random signals like white noise, which is very unpredictable but not structurally complex (Costa *et al* 2005). However, this does not occur with the *AMIFRD*. A steeper decline of the *AMIF* for a given time series (implying a rise in irregularity) does not necessarily point out that physiologic complexity has increased (Goldberger *et al* 2002). However, a decreased irregularity can be found in several diseases (Abásolo *et al* 2008, Gómez *et al* 2007, Jeong *et al* 2001, Hoyer *et al* 2007). Similarly to previous studies, our EEG analysis shows that the *AMIFRD* may characterise biomedical signals acquired under diverse states. Examples of this application are the more negative *AMIFRD* distribution associated with the eyes-closed state in comparison to the eyes-open condition and the differences found between the ictal and non-ictal EEG activities. Furthermore, the use of the *AMIFRD* as a characterising metric in the analysis of experimental recordings has some advantages. Firstly, it can be applied to short time series in comparison to other non-linear classical analysis methods, such as the correlation dimension (Abásolo *et al* 2008, Gómez *et al* 2007, Jeong *et al* 2001). Secondly, the only input parameter for the *AMIF* is the number of histogram partitions (Jeong *et al* 2001, Na *et al* 2002). Finally, the *MI* is invariant under strictly monotone transformations of the input sequences (Pompe *et al* 1998).

It should be noted that, in contrast to other studies (Hoyer *et al* 2005, Quian Quiroga *et al* 2002, Xu *et al* 1997), signals were not embedded in a phase space before computing *MI*. This

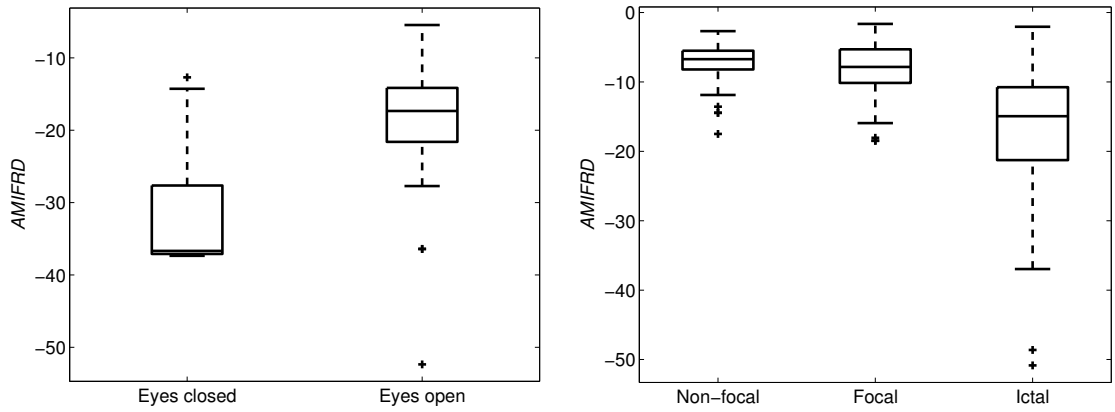

Figure 4. Boxplots representing the distributions of the *AMIFRD* values computed from real EEG signals. (a) Surface EEGs acquired with eyes open and eyes closed. (b) Intracraneal EEG recordings of ictal activity and inter-ictal activity recorded from within the epileptogenic zone and from the opposite brain hemisphere.

embedding should be carried out in order to consider higher dimensional relationships (David *et al* 2004, Pompe *et al* 1998). However, it would require larger signals, something that is not always possible, especially for biological recordings. Additionally, some advanced strategies can be applied to estimate *MI*, like the recursive algorithm by Fraser and Swinney (1986) or the recently proposed techniques by Cellucci *et al* (2005). Nevertheless, we have found that the straightforward computation of the histograms using 32 equal bins after applying a ranking transformation to the data (Pompe *et al* 1998) provided stable estimations of the *AMIFRD*.

5. Conclusions

In recent years, the *AMIFRD* has been widely used in biomedical signal analysis (Abásolo *et al* 2008, Gómez *et al* 2007, Hoyer *et al* 2002, 2005, 2007, Jeong *et al* 2001, Na *et al* 2002, Pompe *et al* 1998). Due to the increasing relevance of the metric in this field, we aimed at gaining a better understanding of the *AMIFRD* in terms of signal processing concepts and at illustrating its application to the signal analysis of biomedical recordings. Hence, we performed a series of simulations where this method was tested using synthetic signals.

Our study has indicated that the *AMIFRD* becomes more negative as the signal is more dominated by white noise. Additionally, noises with wider spectra provide more negative values of the *AMIFRD*, and this parameter is able to detect changes in the non-linear dynamics of a time series. Additionally, we illustrated the application of the *AMIFRD* to real EEGs recorded under different conditions. Nevertheless, it should be noticed that many other non-linear analysis methods are available, and similar studies should be carried out to properly understand the results provided by other analysis techniques.

Acknowledgements

The authors are grateful for the useful feedback of the Referees on the manuscript. They would also like to thank Dr. Andrzejak from the Department of Epileptology at the University of Bonn, Germany, now with the Department of Technology at the University Pompeu Fabra, Spain, for providing the EEG data described in Section 3.4. This study was partially supported by "Ministerio de Educación y Ciencia" and FEDER grant MTM 2005-08519-C02-01 and by the grant project VA108A06 from "Consejería de Educación de la Junta de Castilla y León." J. Escudero was in receipt of an FPU grant from the Spanish Government.

References

Abarbanel H D I, Brown R, Sidorowich J J and Tsimring L Sh 1993 The analysis of observed chaotic data in physical systems *Rev. Mod. Phys.* **65** 1331–92

Abásolo D, Escudero J, Hornero R, Gómez C and Espino P 2008 Approximate entropy and auto mutual information analysis of the electroencephalogram in Alzheimer's disease patients *Med. Bio. Eng. Comput.* **46** 1019–28

Aboy M, Hornero R, Abásolo D and Álvarez D 2006 Interpretation of the Lempel-Ziv complexity measure in the context of biomedical signal analysis *IEEE Trans. Biomed. Eng.* **53** 2282–8

Alonso J F, Mañanas M A, Hoyer D, Topor Z L and Bruce E N 2007 Evaluation of respiratory muscles activity by means of mutual information function at different levels of ventilatory effort *IEEE Trans. Biomed. Eng.* **54** 1573–82

Andrzejak R G, Lehnertz K, Mormann F, Rieke C, David P and Elger C E 2001 Indications of nonlinear deterministic and finite-dimensional structures in time series of brain electrical activity: Dependence on recording region and brain state *Phys. Rev.* E **64** 061907

Baker G L and Gollub J P 1990 *Chaotic Dynamics: an introduction* (Cambridge, UK: Cambridge University Press)

Benedetti F, Arduino D, Costa S, Vighetti S, Tarenzi L, Rainero I and Asteggiano G 2006 Loss of expectation-related mechanisms in Alzheimer's disease makes analgesic therapies less effective *Pain* **121** 133–44

Cellucci C J, Albano A M, Rapp P E 2005 Statistical validation of mutual information calculations: Comparison of alternative numerical algorithms *Phys. Rev.* E **71** 066208

Chapeau-Blondeau F 2007 Autocorrelation versus entropy-based autoinformation for measuring dependence in random signal *Physica* A, **380** 1–18

Costa M, Goldberger A L and Peng C–K 2005 Multiscale entropy analysis of biological signals *Phys. Rev.* E **71** 021906

David O, Cosmelli D and Friston K J 2004 Evaluation of different measures of functional connectivity using a neural mass model *Neuroimage* **21** 659–73

Ferrario M, Signorini M G, Magines G and Cerutti S 2006 Comparison of entropy-based regularity estimators: application to the fetal heart rate signal for the identification of fetal distress *IEEE Trans. Biomed. Eng.* **53** 119–25

Fraser A M and Swinney H L 1986 Independent coordinates for strange attractors from mutual information *Phys. Rev.* A **33** 1134–40

Goldberger A L, Peng C–K and Lipsitz L A 2002 What is physiologic complexity and how does it change with aging and disease? *Neurobiol. Aging* **23** 23–6

Gómez C, Hornero R, Abásolo D, Fernández A and Escudero J 2007 Analysis of the magnetoencephalogram background activity in Alzheimer's disease patients with auto mutual information *Comput. Meth. Programs Biomed.* **87** 239–47

Hinrichs H, Noesselt T and Heinze H-J 2008 Directed information flow – A model free measure to analyze causal interactions in event related EEG–MEG–Experiments *Hum. Brain Mapp.* **29** 193–206

Hornero R, Aboy M, Abásolo D, McNames J and Goldstein B 2005 Interpretation of approximate entropy: analysis of intracranial pressure approximate entropy during acute intracranial hypertension *IEEE Trans. Biomed. Eng.* **52** 1671–80

Hoyer D, Frank B, Baranowski R, Zebrowski J J, Stein P K and Schmidt H 2007 Autonomic information flow rhythms – From heart beat interval to circadian variation *IEEE Eng. Med. Biol. Mag.* **26** 19–24

Hoyer D, Leder U, Hoyer H, Pompe B, Sommer M and Zwiener U 2002 Mutual information and phase dependencies: measures of reduced nonlinear cardiorespiratory interactions after myocardial infarction *Med. Eng. Phys.* **24** 33–43

Hoyer D, Pompe B, Chon K H, Hardraht H, Wicher C and Zwiener U 2005 Mutual information function assess autonomic information flow of heart rate dynamics at different time scales *IEEE Trans. Biomed. Eng.* **52** 584–92

Huang L, Yu P, Ju F and Cheng J 2003 Prediction of response to incision using mutual information of electroencephalograms during anaesthesia *Med. Eng. Phys.* **25** 321–7

Jeong J, Gore J C, Peterson B S 2001 Mutual information analysis of the EEG in patients with Alzheimer's disease *Clin. Neurophysiol.* **112** 827–35

Kantz H and Schreiber T 1997 *Nonlinear Time Series Analysis* (Cambridge, UK: Cambridge University Press)

Min B–C, Jin S–H, Kang I–H, Lee D H, Kang J K, Lee S T and Sakamoto K 2003 Analysis of mutual information content for EEG responses to odor stimulation for subjects classified by occupation *Chem. Senses* **28** 741–9

Na S H, Jin S–H, Kim S Y and Ham B–J 2002 EEG in schizophrenic patients: mutual information analysis *Clin. Neurophysiol.* **113** 1954–60

Palacios M, Friedrich H, Götze C, Vallverdú M, Bayes de Luna A, Caminal P and Hoyer D 2007 Changes of autonomic information flow due to idiopathic dilated cardiomyopathy *Physiol. Meas.* **28** 677–88

Paluš M 1996 Coarse-grained entropy rates for characterization of complex time series *Physica* D **93** 67–77

Paluš M, Albrecht V and Dvořák I 1993 Information theoretic test for nonlinearity in time series *Phys. Lett.* A **175** 203–9

Pincus S M 1991 Approximate entropy as a measure of system complexity *Proc. Natl. Acad. Sci. USA* **88** 2297–2301

Pompe B, Blidh P, Hoyer D and Eiselt M 1998 Using mutual information to measure coupling in the cardiorespiratory system *IEEE Eng. Med. Biol. Mag.* **17** 32–9

Quian Quiroga R, Kraskov A, Kreuz T and Grassberger P 2002 Performance of different synchronization measures in real data: A case study on electroencephalographic signals *Phys. Rev.* E **65** 041903

Rapp P E, Cellucci C J, Watanabe T A A and Albano A M 2005 Quantitative characterization of the complexity of multichannel human EEGs *Int. J. of Bifurcation and Chaos* **15** 1737–44

Shannon C E and Weaver W 1949 *The Mathematical Theory of Communication* (Urbana, IL: University of Illinois Press)

Teplan M, Krakovská A and Štolc S 2006 EEG responses to long-term audio–visual stimulation *Int. J. Psychophysiol.* **59** 81–90

Watanabe T A A, Cellucci C J, Kohegyi E, Bashore T R, Josiassen R C, Greenbaun N N and Rapp P E 2003 The algorithmic complexity of multichannel EEGs is sensitive to changes in behavior *Psychophysiol.* **40** 77–97

Xu J, Liu Z, Liu R and Yang Q 1997 Information transmission in human cerebral cortex *Physica* D **106** 363–74